

# Topology optimized mode multiplexing in silicon-on-insulator photonic wire waveguides

LOUISE F. FRELLSEN,<sup>1,\*</sup> YUNHONG DING,<sup>1</sup> OLE SIGMUND,<sup>2</sup> AND LARS H. FRANDSEN<sup>1</sup>

<sup>1</sup>DTU Fotonik, Department of Photonics Engineering, Technical University of Denmark, 2800 Lyngby, Denmark

<sup>2</sup>DTU Mekanik, Department of Mechanics Engineering, Technical University of Denmark, 2800 Lyngby, Denmark

\*louifr@fotonik.dtu.dk

**Abstract:** We design and experimentally verify a topology optimized low-loss and broadband two-mode (de-)multiplexer, which is (de-)multiplexing the fundamental and the first-order transverse-electric modes in a silicon photonic wire. The device has a footprint of 2.6 μm x 4.22 μm and exhibits a loss <1.2 dB in a 100 nm bandwidth measured around 1570 nm. The measured cross talk is <-12 dB and the extinction ratio is >14 dB in the C-band. Furthermore, we demonstrate that the design method can be expanded to include more modes, in this case including also the second order transverse-electric mode, while maintaining functionality.

©2016 Optical Society of America

**OCIS codes:** (000.3860) Mathematical methods in physics; (000.4430) Numerical approximation and analysis; (030.4070) Modes; (050.6624) Subwavelength structures; (130.3120) Integrated optics devices.

## References and links

1. R. Kirchain and L. Kimerling, "A roadmap for nanophotonics," *Nat. Photonics* **1**(6), 303–305 (2007).
2. Y. Ding, J. Xu, F. Da Ros, B. Huang, H. Ou, and C. Peucheret, "On-chip two-mode division multiplexing using tapered directional coupler-based mode multiplexer and demultiplexer," *Opt. Express* **21**(8), 10376–10382 (2013).
3. Z. Zhang, X. Hu, and J. Wang, "On-chip optical mode exchange using tapered directional coupler," *Sci. Rep.* **5**, 16072 (2015).
4. J. D. Love and N. Riesen, "Single-, few- and multimode Y-Junctions," *J. Lightwave Technol.* **30**(3), 304–309 (2012).
5. J. B. Driscoll, R. R. Grote, B. Souhan, J. I. Dadap, M. Lu, and R. M. Osgood, "Asymmetric Y junctions in silicon waveguides for on-chip mode-division multiplexing," *Opt. Lett.* **38**(11), 1854–1856 (2013).
6. Y. Kawaguchi and K. Tsutsumi, "Mode multiplexing and demultiplexing devices using multimode interference couplers," *Electron. Lett.* **38**(25), 1701–1702 (2002).
7. D. Pérez-Galacho, D. Marras-Morini, A. Ortega-Moñux, J. G. Wangüemert-Pérez, and L. Vivien, "Add/drop mode-division multiplexer based on a Mach-Zender interferometer and periodic waveguides," *IEEE Photonics J.* **7**(4), 7147861 (2015).
8. L.-W. Luo, N. Ophir, C. P. Chen, L. H. Gabrielli, C. B. Poitras, K. Bergmen, and M. Lipson, "WDM-compatible mode-division multiplexing on a silicon chip," *Nat. Commun.* **5**, 3069 (2014).
9. M. P. Bendsøe and N. Kikuchi, "Generating optimal topologies in structural design using a homogenization method," *Comput. Methods Appl. Mech. Eng.* **71**(2), 197–224 (1988).
10. P. I. Borel, B. Bilenberg, L. H. Frandsen, T. Nielsen, J. Fage-Pedersen, A. V. Lavrinenko, J. S. Jensen, O. Sigmund, and A. Kristensen, "Imprinted silicon-based nanophotonics," *Opt. Express* **15**(3), 1261–1266 (2007).
11. L. H. Frandsen, Y. Elesin, L. F. Frellsen, M. Mitrovic, Y. Ding, O. Sigmund, and K. Yvind, "Topology optimized mode conversion in a photonic crystal waveguide fabricated in silicon-on-insulator material," *Opt. Express* **22**(7), 8525–8532 (2014).
12. L. H. Frandsen, Y. Elesin, O. Sigmund, and K. Yvind, "Topology optimization of coupled photonic crystal cavities for flat-top drop filter functionality," in *2015 CLEO Europe*, (OSA, 2015), paper CK\_9\_1.
13. J. S. Jensen and O. Sigmund, "Topology optimization for nano-photonics," *Laser Photonics Rev.* **5**(2), 308–321 (2011).
14. J. Lu and J. Vučković, "Nanophotonic computational design," *Opt. Express* **21**(11), 13351–13367 (2013).
15. J. Lu and J. Vučković, "Objective-first design of high-efficiency, small-footprint couplers between arbitrary nanophotonic waveguide modes," *Opt. Express* **20**(7), 7221–7236 (2012).
16. A. Y. Piggot, J. Lu, K. G. Lagoudakis, J. Petykiewicz, T. M. Babinec, and J. Vuckovic, "Inverse design and demonstration of a compact and broadband on-chip wavelength demultiplexer," *Nat. Photonics* **9**, 347–377 (2015).

17. B. Shen, P. Wang, R. Polson, and R. Menon, "An integrated-nanophotonics polarization beamsplitter with  $2.4 \times 2.4 \mu\text{m}^2$  footprint," *Nat. Photonics* **9**(6), 378–382 (2015).
18. O. Sigmund, J. S. Jensen, and L. H. Frandsen, "On nanostructured silicon success," *Nat. Photonics* **10**(3), 142–143 (2016).
19. Y. Elesin, B. S. Lazarov, J. S. Jensen, and O. Sigmund, "Design of robust and efficient photonic switches using topology optimization," *Photon. Nanostruct. Fundam. Appl.* **10**(1), 153–165 (2012).
20. Y. Elesin, B. S. Lazarov, J. S. Jensen, and O. Sigmund, "Time domain topology optimization of 3D nanophotonic devices," *Photon. Nanostruct. – Fundam. Appl.* **12**, 23–33 (2014).

## 1. Introduction

The increasing capacity demand for optical fiber communication networks has led to the investigation of space division multiplexing (SDM) as a possible solution to the predicted capacity crunch of the internet. Meanwhile, the field of photonic integrated circuits (PICs) will allow for high device densities while requiring relatively low operating power [1] and supporting cheap, robust, and effective optical communication systems. Recently on-chip mode-division-multiplexing (MDM) has gained significant attention as an integrated SDM technique, thanks to the possibility of routing multiplexed optical signals on a sub-mm scale, in which the footprint of the planar circuits could potentially be reduced [1–5]. Therefore, efficient mode (de-)multiplexers are under investigation being essential components for MDM. Integrated mode multiplexers have typically been relying on asymmetric directional couplers [2,3], Y-junctions [4,5], or multimode interferometers [6,7]. Although these solutions have proved to be promising, they deliver device footprints in the range of tens to hundreds of  $\mu\text{m}^2$  for a two-mode multiplexer. Increasing the number of modes to be multiplexed increases the device sizes substantially, as the commonly employed scheme in this respect is cascading designs (see e.g [8].)

**Topology optimization (TO)** is a general and robust inverse design tool [9] used for creating numerous different nanophotonic components with e.g. low losses, exotic functionalities, and controllable bandwidth [10–13]. Recently Lu and Vuckovic [14,15] have proposed a very similar optimization technique entitled the "**objective-first method**". Although convergence behavior may be different, there is, so far, no evidence of either of the approaches being superior to the other. **Depending on parameter settings and feature size, the two approaches may converge to different local minima of the highly non-convex optimization problems.** The approach from [14,15] as well as an alternative approach were recently highlighted in *Nature Photonics* [16,17] and commented upon in a corresponding Letter to the Editor by the authors [18]. In this paper, we present a topology optimized design of a low-loss broadband (de-)multiplexer multiplexing the transverse-electric fundamental even mode ( $\text{TE}_0$ ) and the first-order odd mode ( $\text{TE}_1$ ) in a silicon photonic wire. We verify the design by fabrication in silicon-on-insulator (SOI) material and record mode profiles and spectra to measure the functionality and efficiency of the device. Furthermore, a three-mode (de-)multiplexer design, including the second-order even mode ( $\text{TE}_2$ ), is realized to demonstrate the potential of employing the TO method to create compact many-mode SDM components for PICs.

## 2. Design, optimization, and modelling

### 2.1 Topology optimization of a two-mode de-multiplexer

Topology optimization is applied to a silicon (white) structure shown in Fig. 1(a) with a  $2.4 \mu\text{m} \times 4 \mu\text{m}$  rectangular region having a double-mode input waveguide supporting the  $\text{TE}_0$  (red) and the  $\text{TE}_1$  (blue) modes. The objective of the TO is to obtain a design that demultiplexes a combined  $\text{TE}_0 + \text{TE}_1$  signal transmitted from the input waveguide to the two single-mode output waveguides. The  $\text{TE}_1$  (blue) signal should be converted to a  $\text{TE}_0$  signal in the lower of the two output waveguides while the input  $\text{TE}_0$  (red) signal should be directed to the upper waveguide as sketched in Fig. 1(a). The input waveguide is shifted vertically towards the upper output waveguide to allow a smooth path for the input  $\text{TE}_0$  mode to the

upper output waveguide. The  $TE_0$  and the  $TE_1$  modes are excited as Gaussian pulses, separated by a time delay of 400 fs, at position A (orange) in Fig. 1(a) having spectral bandwidths (full-width half-maximum) of  $\sim 260$  nm centered at  $\sim 1580$  nm. In the optimization, the design objective is to de-multiplex the two pulses to the separate output waveguides while keeping the amplitudes and widths of the input pulses. This is achieved by estimating the arrival time of the two pulses and optimizing for having a strong signal in the corresponding output waveguide and minimizing the intensity in the opposite waveguide. Three dimensional (3D) TO is done using a software package developed in-house [19,20] utilizing 3D finite-difference time-domain (FDTD) calculations combined with sensitivity analysis. The gradient calculations are performed extremely efficiently using the so-called adjoint approach, cf [13]. This means that, independent on the number of design variables, analytical gradients can be computed at the cost of one extra backward FDTD time integration per objective function. The details of the adjoint approach can be found in [19]. To fulfill the objective of the TO, iterative material redistribution is performed in the design domain (yellow) in Fig. 1(a) having a size of  $2.6 \mu\text{m} \times 4.22 \mu\text{m}$  and being slightly larger than the square silicon region. The 340 nm thick silicon device layer has a permittivity of  $\epsilon_{\text{Si}} = 11.68$  and is placed on top of a silica buffer layer with a permittivity of  $\epsilon_{\text{silica}} = 2.085$  with air above. Throughout the optimization, the designed structures in the silicon layer are constrained to be uniform in the vertical direction to render fabrication feasible. The optimization is performed with a 32 nm spatial resolution in a mesh of  $280 \times 110 \times 20$  grid points and perfectly matched absorbing layers as boundaries. The converged topology optimized structure obtained after 200 iterations, taking  $\sim 8$  hours on 112 CPUs (XeonE5-2665 cores connected with infini-band), is shown in Fig. 1(b); the smallest features have a width of a single pixel these are, however, found to have only inferior effects on the performance and could have been filtered out during optimization by choosing different filtering parameters in the TO and/or running more iteration steps. For the current design, it should be stressed that no thorough investigations have been made of the filtering parameters in order to make the design and the objectives converge more efficiently. The final design is obtained as an image file. Upon extraction to the design software a simple threshold filtering is taking place converting any greyscale pixel to be either black or white.

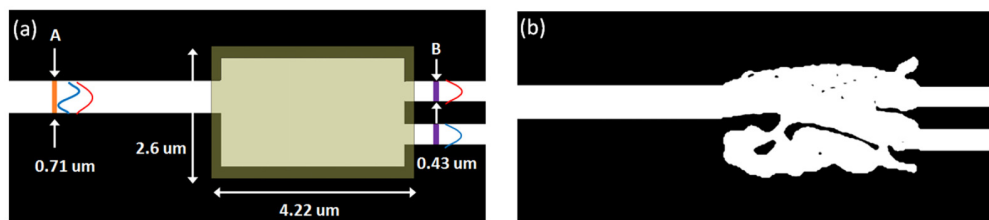


Fig. 1. (a) Initial structure for the TO with regions of silicon (white) and air (black). Yellow indicates the used design domain, orange the position of the source and purple the positions of the objectives. (b) The mode de-multiplexer obtained after 200 iteration steps of 3D TO.

## 2.2 Modelling the topology optimized structures

The optimized design shown in Fig. 1(b) is verified by 3D FDTD calculations where two  $TE_0$  modes are input in the upper and lower single mode waveguides (being the output waveguides in Fig. 1(a)) and measuring the transmitted power to the double-mode waveguide, i.e. simulating the device in a multiplexing configuration. Figure 2(a) shows the out-of-plane H-field ( $H_z$ ) at 1580 nm calculated for both  $TE_0$  signals transmitted through the mode multiplexer. As intended, the signal originating from the upper waveguide maintains the fundamental  $TE_0$  mode profile while the signal from the lower waveguide is converted to the  $TE_1$  mode in the double mode waveguide. The mechanism allowing for the mode conversion is based on sophisticated scattering processes and is very different from conventional

interference and adiabatic conversion mechanisms due to the small scale enforced in the optimization. Only a small fraction of the field seems to be contained in the lower part of the structure and one could question the significance of this ‘appendix’. To investigate this, simulations were made on a design where the ‘appendix’ had been manually removed as shown along with the field simulations in Fig. 2(b). The calculated fluxes and transmissions with (red/blue) and without (magenta/cyan) the ‘appendix’ are shown in Figs. 2(c) and 2(d), respectively. From these it is clear that the appendix is of relevance to the performance as the losses are increased when the ‘appendix’ is removed. It is however of note, that the functionality remains in its absence which indicates the potential of obtaining an even more compact device by doing further re-optimization with a structure like Fig. 2(b) as input. The extinction ratio of the full design is calculated as the difference between the value of the valley of the  $TE_1$  mode and the highest value of the lowest of the two peaks, it is found to be  $>18$  dB at 1580 nm. The conversion loss is  $<1$  dB in the bandwidth of the source from 1450 nm to 1700 nm.

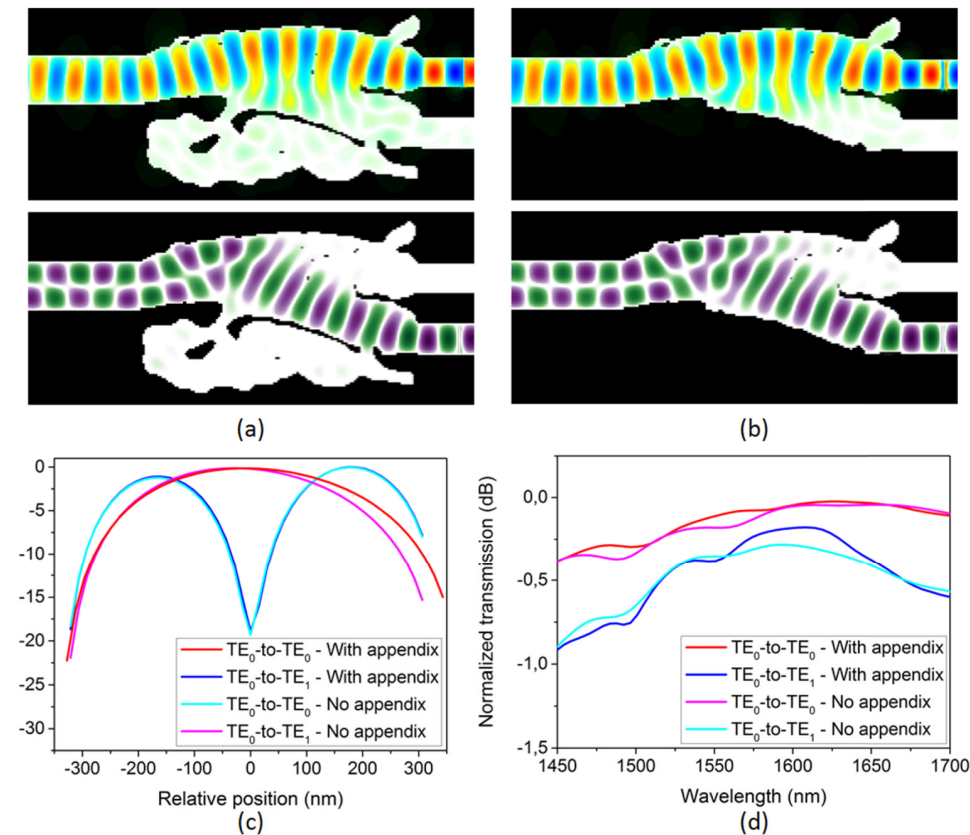


Fig. 2. (a) Propagation of the  $H_x$ -field through the topology optimized structure at a wavelength of 1580 nm. (b) Similar field simulations through the structure with the ‘appendix’ manually removed from the design. (c) 3D FDTD-calculated power flux of the two  $TE_0$  modes originating in the single mode waveguides and multiplexed to the  $TE_0$  and the  $TE_1$  mode for the full (red/blue) and altered (magenta/cyan) designs, calculated at 1580 nm. (d) The corresponding 3D FDTD-calculated transmission properties of the devices as a function of wavelength normalized to the transmission in a straight photonic wire.

### 3. Experimental results

#### 3.1 Fabrication

The topology optimized mode multiplexer was fabricated in SOI material having an ~340 nm thick silicon layer on top of an ~2000 nm thick silica buffer layer. The two structures illustrated in Fig. 3(a) were fabricated to characterize the conversion and transmission properties of the multiplexer. The first structure (S1) inputs the  $TE_0$  mode in either of the input waveguides and the output signal is sent to a vertical grating coupler allowing recording the output mode profiles. The second structure (S2) is constructed from two mode multiplexers, one being mirrored and placed ~9  $\mu\text{m}$  after the other in order to de-multiplex a multiplexed signal. This is done to accommodate our present measurement set-up in which we cannot effectively collect a first-order mode but are restricted to collect fundamental modes. As the design is reversible and characterized in the linear regime, the loss of a single multiplexer device can be estimated by halving the measured insertion loss.

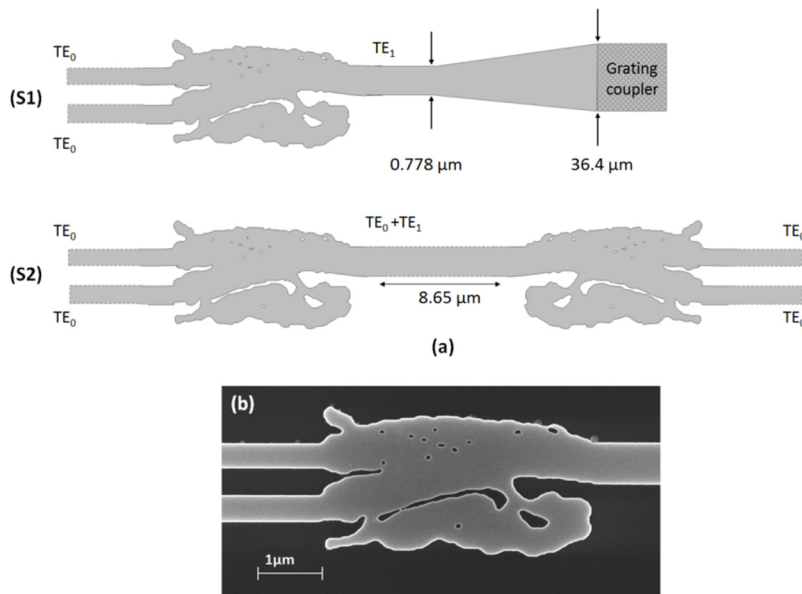


Fig. 3. (a) Sketches of the two fabricated S1 (top) and S2 (bottom) structures (not to scale). The S1 structure inputs a  $TE_0$  mode in either of the input waveguides and sends the output signal to a grating coupler over which an infrared camera is placed to allow recording of the output mode profile. The S2 structure lets the input signals undergo multiplexing and de-multiplexing allowing for characterization of the insertion loss of the single multiplexer. (b) Scanning electron microscope image of the fabricated (de-)multiplexer structure.

The designs were defined in an ~110 nm thick layer of positive electron beam resist (ZEP520A) by using a JEOL JBX-9500FS electron-beam lithography system. The system was operated at 100 keV and the writing field of the machine was 0.5 mm x 0.5 mm. The estimated diameter of the electron beam is 6 nm and it is scanned in steps of 4 nm. Proximity error correction was applied to account for backscattered electrons. The developed resist is used as a soft mask for inductively coupled plasma reactive ion etching using  $SF_6$  and  $C_4F_8$  gases. As a final step SU-8 polymer waveguides were defined to overlap with inversely tapered silicon in- and out-put waveguides utilized for optimizing the coupling from tapered lenses fibers. Figure 3(b) shows a scanning electron micrograph (SEM) image of the fabricated structure confirming that the design is transferred successfully to the silicon.

### 3.2 Characterization of the topology optimized mode converters

To experimentally verify the functionality of the device, the S1 structure illustrated in Fig. 3(a) is used for recording the mode profiles of the multiplexer as light is coupled into either the upper or lower waveguide. The output waveguide, carrying the multiplexed signal, is gently tapered from 778 nm to 36.4  $\mu$ m where it ends in a vertical grating coupler. The signal is thus coupled out of plane and collected by a microscope above which an InGaAs infrared camera (IR-Cam – Xenics XEVA XC130) is placed to image the mode profile. If the original  $TE_0$  mode has been coupled to the upper arm, it shall remain a  $TE_0$  mode when traversing the multiplexer, whereas light coupled to the lower arm will have been converted to a  $TE_1$  mode before reaching the IR camera. Figure 4(a) shows the recorded mode profiles at 1530 nm, 1570 nm, and 1610 nm. The upper/lower row is recorded for an input signal to the upper/lower port of the multiplexer, respectively. As expected, the output signal from the upper/lower port is seen to be  $TE_0/TE_1$  modes, respectively. Mode conversion for the lower input port was seen in the entire wavelength range (1520 nm – 1620 nm) of the laser used in the experiment. Figure 4(b) shows the sampled cross-section of the mode profiles of the two modes recorded at 1570 nm. The  $TE_1/TE_0$  extinction ratio for light input from the lower port was measured to be  $\sim$ 17 dB at 1570 nm. In the C-band the measured extinction ratio is larger than 14 dB. This value is expected to be limited by the image resolution of the measurement setup as only few pixels define the steep valley of the  $TE_1$  signal.

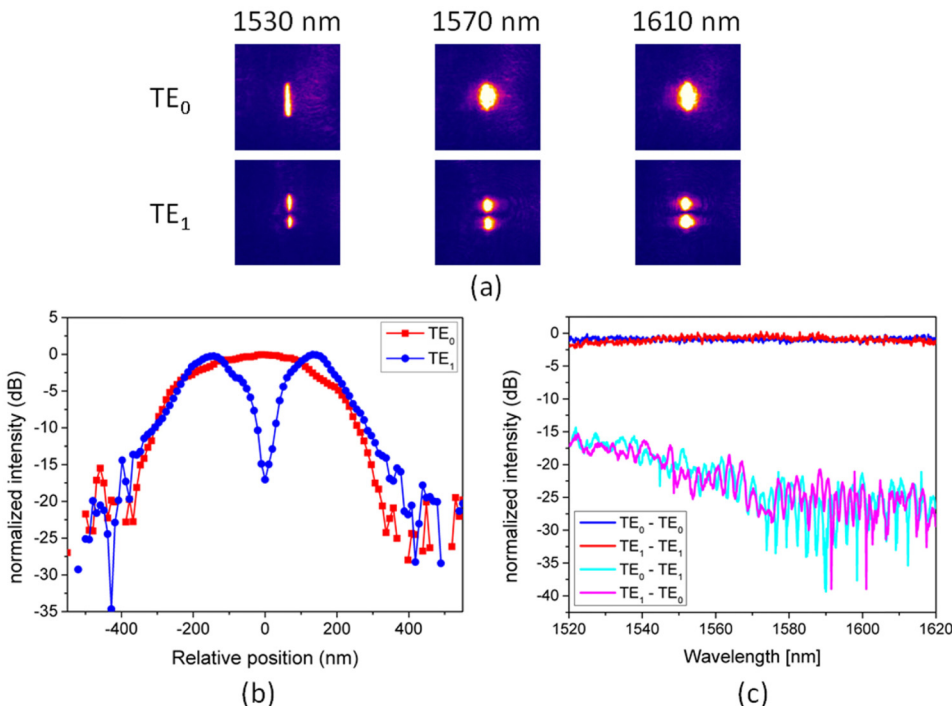


Fig. 4. (a) Mode profiles of the topology optimized mode multiplexer measured using the structure S1 shown in Fig. 3. (b) Line scans across the mode profiles recorded at 1570 nm when light is input in the upper (red) or lower arm (blue). (c) Transmission spectra for the mode multiplexer measured from the structure S2 shown in Fig. 3. All spectra are normalized to the transmission through a straight waveguide.

Transmission spectra were recorded for light travelling through all four possible channel combinations of the input and output waveguides of structure S2 where the light is multiplexed and subsequently de-multiplexed. The transmission spectra were recorded in the wavelength region of 1520 nm to 1620 nm and have been normalized to the spectrum of a

straight waveguide. As the design is reversible and characterized in the linear regime the loss of a single multiplexer device can be estimated by halving the measured losses reported in Fig. 4(c). The insertion loss is found to be <1.2 dB for the entire 100 nm region of the source with a cross-talk <-12 dB.

#### 4. Three-mode multiplexer

To investigate the applicability of TO to structures (de-)multiplexing a higher number of modes without a substantial increase in the device footprint, a design was made based on the same principle as described for the two-mode (de-)multiplexer. The structure was expanded to include three single mode waveguides supporting only the  $TE_0$  mode to be multiplexed onto a wider output waveguide, see Fig. 5(a). The design domain has a size of  $6.08 \mu\text{m} \times 4.93 \mu\text{m}$ . As before, the objective of the TO is to de-multiplex/convert the  $TE_0$ ,  $TE_1$ , and  $TE_2$  signals from the input waveguide to  $TE_0$  modes in each of the three single-mode output waveguides.

The conditions of the optimization were identical to those described for the two-mode multiplexer in section 2.1 and the structure was fabricated in the same manner, as described in section 3.1. An SEM image of the optimized structure with overlaid mode profiles calculated with 3D FDTD is presented in Fig. 5(b). Two designs similar to S1 and S2 of Fig. 3(a) were fabricated allowing for analogous types of characterizations.

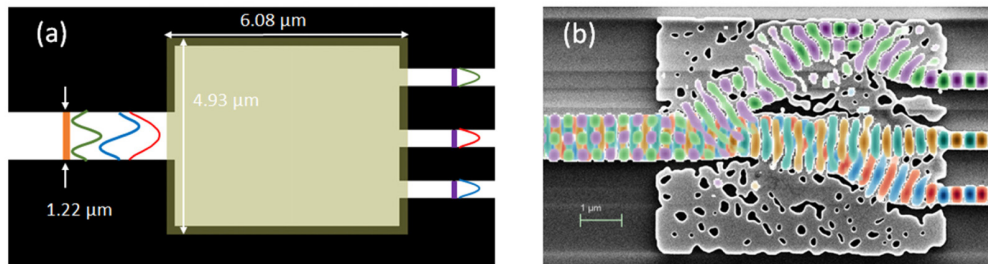


Fig. 5. (a) Initial structure for the TO of a 3-mode multiplexer. The design domain is indicated in yellow while the positions of the excitations is indicated in orange and those of the objectives in purple. (b) SEM image of the fabricated optimized structure, overlaid with a 3D FDTD-calculation of the  $H_z$ -field of the structure.

Functionality and performance of the device was experimentally verified by recording the mode profiles shown in Fig. 6(a); clearly, multiplexing and mode conversion takes place for all channels. The loss was investigated for a mirrored structure inputting the  $TE_0$  mode in any of the three channels, multiplexing it and then recording the subsequently de-multiplexed  $TE_0$  mode. Spectra for all possible paths of the light through this mirrored structure are given in Fig. 6(b). The 3 dB bandwidth is  $\sim 80$  nm with lowest loss around 1.7 dB. Within the C-band the measured extinction ratio for the  $TE_1$  mode is  $> 14$  dB. The image resolution is, however, too limited to obtain a proper estimate for the extinction ratio of the  $TE_2$  mode. Here, it has been the goal to demonstrate the possibility of realizing few-mode (de-)multiplexing devices utilizing TO rather than to investigate the optimum design attainable, which will in turn be a trade-off between the size and the functionality. However, we believe that the performance figures would be possible to improve through further optimizations with altered parameters to obtain a device converging to a local minimum with lower losses and cross-talks of the various channels.

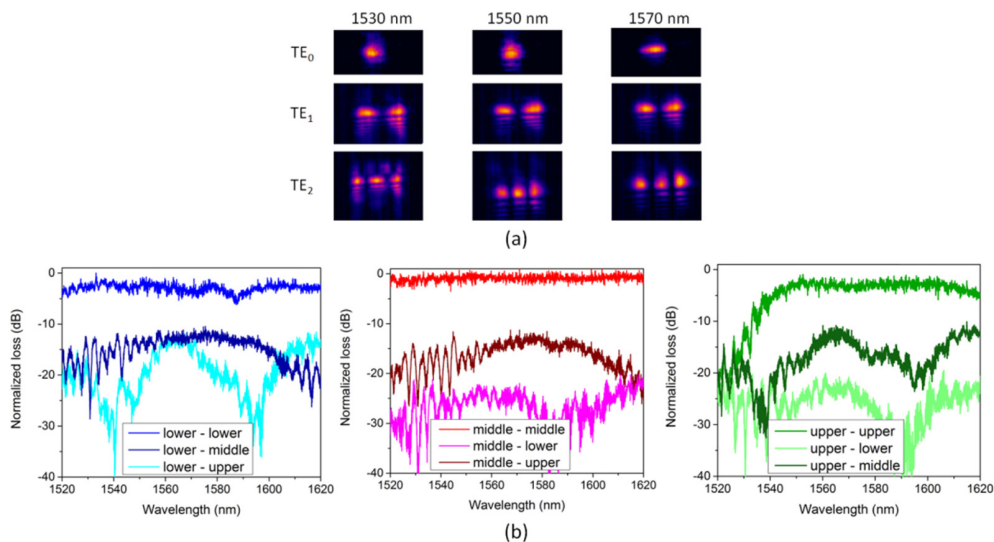


Fig. 6. Experimental results for the three-mode multiplexer. (a) Mode profiles recorded using a vertical grating coupler and an IR camera collected at three different wavelengths. (b) Transmission spectra for a multiplexer and de-multiplexer configuration. The legends refer to the position of the input/output waveguides, ‘lower’ carries the de-multiplexed TE<sub>1</sub> mode, ‘middle’ the TE<sub>0</sub> and ‘upper’ the TE<sub>2</sub> mode.

## 5. Conclusion

We have demonstrated the utilization of topology optimization for the design of a mode (de-)multiplexer operating on the fundamental and the first-order transverse-electric modes having an ultra-compact footprint of  $2.6 \mu\text{m} \times 4.22 \mu\text{m}$ . It is more compact than any previous reported device without a loss of the general functionality. The optimized designs were fabricated in silicon-on-insulator material using e-beam lithography; mode profiles were recorded demonstrating the functionality of the device. The extinction ratio was measured to be  $>14$  dB in the C-band with insertion losses  $<1.2$  dB in a bandwidth of 100 nm limited by the available laser source. The crosstalk measured for a multiplexer followed by a de-multiplexer was less than  $-12$  dB.

In addition, a (de-)multiplexer including the second-order transverse electric mode was designed with a footprint increased to no more than  $6.08 \mu\text{m} \times 4.93 \mu\text{m}$ ; it experimentally performed in a bandwidth of  $\sim 80$  nm with lowest losses of  $\sim 1.7$  dB. We believe that the performance figures can be improved through further optimizations, but here we have demonstrated that the technique can be expanded to include more modes so that the topology optimization method can be employed to create ultra-compact mode (de-)multiplexers for multiple modes required for photonic integrated components.

## Funding

This work was supported by the VILLUM foundation via the project ‘Optical Nano-engineered Components for High-capacity Integrated silicon Photonics’ (ONCHIP).